

Comparison of Thermophysical Properties of PIM Feedstocks with Polyoxymethylene and Wax-Polyolefin Binders

Alexander N. Muranov ^{1*}, Maxim A. Kocharov ¹, Maxim S. Mikhailov ¹

¹ *Institute of Design-Technology Informatics, Russian Academy of Sciences, Russian Federation.*

Received 22 February 2024; Revised 17 May 2024; Accepted 21 May 2024; Published 01 June 2024

Abstract

One of the high-performance technologies for the serial production of small-sized metal and ceramic complex-profile parts is powder injection molding (PIM). The most industrially demanded types of polymer binder in PIM technology are polyoxymethylene-based compositions and wax-polyolefin mixtures. Despite the large number of studies devoted to different compositions of polymer binder for PIM technology, the actual task is still a comparative analysis of the properties of different binder types to determine their advantages and disadvantages, as well as the optimization of the used compositions. In this regard, this study aims at a comparative analysis of the thermophysical properties of the most demanded feedstocks with binder based on polyoxymethylene and wax-polyolefin mixtures under the condition of using identical steel powder filler. The specific heat capacity, temperatures, and heat of phase transitions, as well as the thermal inertia and effective thermal conductivity of the compared types of feedstocks, were determined as a result of the calculation-experimental study. The obtained data can replenish the knowledge bases necessary for simulation modeling and optimizing powder molding processes of various products made of 42CrMo4 steel. As a result of a comparative analysis of the thermophysical properties of feedstocks with identical powders, the kinetic effects in the thermal processes of forming feedstocks with polyoxymethylene are less significant than those in analogs with wax-polyolefin binder, which facilitates their moldability. Thus, the feedstock with polyoxymethylene has a significantly higher rate of temperature field leveling than the analogs with wax-polyolefin binder. Because of the insignificant difference in specific heat capacity, feedstocks based on polyoxymethylene have 1.5 times higher effective thermal conductivity and approximately 20% higher thermal inertia than feedstocks with identical powder filler and binder in the form of a wax-polyolefin mixture. The technological advantages of feedstocks with a wax-polyolefin binder include the possibility of processing at lower temperatures.

Keywords: Thermophysical Properties; Powder-Polymer Mixture; Powder Injection Molding; Polyoxymeth-Ylene; Polyolefins; Waxes.

1. Introduction

The most effective technologies for the production of small-sized metal complex-profile parts today are metal injection molding (MIM), additive manufacturing (AM); in ceramic products, technologies of slip casting and powder injection molding (PIM), including low-pressure hot molding (LP PIM) [1]. By combining the productivity of injection molding with the versatility of sintering the powder charge with the required composition, Powder Injection Molding (PIM) technologies combine the advantages of traditional powder metallurgy methods and casting into metal molds. In contrast to additive technologies, injection molding of powder-polymer blends allows for the efficient mass production of precise, small, and complex parts at optimal cost and with a given set of properties. In addition, these technologies are efficient enough to produce small parts of complex configurations from difficult-to-machine materials.

* Corresponding author: alexander.n.muranov@yandex.ru

<http://dx.doi.org/10.28991/CEJ-2024-010-06-05>



© 2024 by the authors. Licensee C.E.J, Tehran, Iran. This article is an open access article distributed under the terms and conditions of the Creative Commons Attribution (CC-BY) license (<http://creativecommons.org/licenses/by/4.0/>).

PIM uses a dispersed-filled composite material in the form of a mixture of polymer binder and powders, known as the "feedstock", followed by molding of the product by injecting this mixture into the cavity of the mold, curing of the casting, removal of the cured casting (the "green" part is the powder-filled polymer), removal of the polymer binder (debinding), followed by sintering of the porous powder part (the "brown" part), resulting in a "finished" part. If necessary, the sintered part undergoes a final mechanical and chemical-thermal treatment. In the case of the catalytic debinding process, the polyoxymethylene-based binder is removed from the green part in nitric acid vapors in a special furnace used for further sintering of powdered part blanks. In the case of wax-polypropylene blends for the solution-thermal method, the wax is washed out from the preform by a non-polar solvent, which leaves behind a developed system of interconnected porosities. The system of pores formed as a result of solution debinding during the subsequent heating ensures unhindered escape of the gaseous pyrolysis products of the polyolefin component of the polymer blend, which, depending on the type of polyolefin, account for more than 99.91% of its initial mass or the mass fraction of ash, which is less than 0.09% and has virtually no effect on the chemical composition of the sintered material. Such a two-stage technology of binder removal from the preform prevents the appearance of cracks and local heterogeneities in the body of the sintered "brown" powder part and ensures the preservation of its geometry.

The relevant scientific and technical literature presents a more detailed description of the PIM technology and the processed and final materials [1] and does not appear here to reduce the scope of the work.

It is essential that the wide range of combinations possible between the dispersed filler and the polymer blend of the binder results in a significant quantitative and qualitative difference in the properties of the feedstocks, which determine the technological modes of their processing and, to a large extent, the quality of the final product—parts mass produced by the PIM method. Polyoxymethylene, ethylene vinyl acetate, polystyrene, polyethylene glycol, polymethyl methacrylate, polyolefins in the form of polypropylene, polyethylene, and other polymers and oligomers are the main components of the binder [2-4]. However, the most industrially demanded types of polymer binder in PIM technology are polyoxymethylene-based composition and wax-polyolefin mixture [3-5]. Despite a large number of research and experimental and technological works devoted to different compositions of polymer binder for PIM technology, the actual task is still a comparative analysis of the properties of different types of binder to determine their advantages and disadvantages and to optimize the compositions used. Here, the rheological and thermophysical properties of feedstock, its PVT characteristics, and compactability are the main properties determining the molding modes of part blanks.

Since the process of forming feedstocks, like any dispersed-filled thermoplastics, is determined mainly by their rheological properties and their ability to compact under pressure, numerous studies have been devoted to the study of these properties [6-8]. At the same time, the determination of the thermophysical characteristics of feedstock is carried out mainly to clarify the temperature ranges of processing and to use the obtained thermophysical characteristics for a specific feedstock composition when simulating and optimizing its casting modes using appropriate software. However, differences in the composition and properties of the polymer binder have a significant impact not only on the compaction and rheological properties of feedstocks but also on their thermal conductivity, heat capacity, and thermal inertia. An analysis of the literature shows that there is, for example, a study [9] on a comparative study of the compaction of feedstocks with the same powder filler and various most popular types of binders, but similar results of a comparative study of thermophysical properties are not presented in the literature. Thus, such a comparative analysis of thermophysical properties is an urgent task, the results of which will allow technologists to provide additional recommendations on the use of one or another type of binder in feedstocks. In this regard, this study aims at a comparative analysis of the thermophysical properties of the most demanded feedstocks with a binder based on a polyoxymethylene and wax-polyolefin mixture using an identical powder filler.

2. Literature Review

Recently, the application of PIM technology has expanded from the production of complex profile parts to the production of critical-duty loaded parts made of various materials. The flexibility of technological capabilities provided by PIM technology not only increases the economic efficiency of production but also contributes to the quality of the final product, which predetermines the development and spread of this technology. Nevertheless, the quality of products produced by the MIM method is contingent on the properties of the used feedstock and the modes of multistage technology employed in its processing. The feedstock binder must function as a flowing and transporting medium at a high-volume fraction of powder filler during mixing and injection molding. The binder should wet the powder well for quality mixing, provide high strength to the semi-finished product (green part), and prevent segregation during molding. After molding, the binder should be removed without compromising the part integrity, maintaining the strength of the semi-finished product, called the brown part, and avoiding adverse effects on the final composition, structure, and material properties of the sintered part [10-12].

For the first approximation, the casting material called feedstock can be a two-component dispersed-filled composite. However, the polymer dispersion medium is much more complex, and the use of several components that generally form a polymer blend provides the required combination of polymer binder properties [13-15]. Other factors that

determine the feedstock casting possibility are the volume fraction, size, and geometry of the powder particles. Feedstock production uses both charges of metal powders and powders of finished alloys or master alloys of precise or enriched compositions as dispersed metal components. Producing ceramic parts requires a charge of ceramic powders with the necessary sintering or other additives. The multitude of potential combinations between dispersed fillers and polymer blends of binders gives rise to a notable disparity in the intrinsic characteristics of the feedstocks, which, in turn, requires the analysis of their characteristics to determine the optimal technological modes of processing feedstocks into products [15-17] and to determine the advantages and disadvantages of the corresponding binder compositions. As mentioned, the main properties determining the modes of feedstock formation should include their rheological and thermophysical properties, PVT characteristics, and compactability. As an example, we note that the results of [9] show that feedstocks with the same powder filler and different types of binders have a 1.5-fold difference in compaction ability at the molding stage. Thus, the type of polymer binder has a significant impact on the main technological properties of the feedstock, which determine its ability to be molded. The type of polymer binder, among other things, has a significant impact on the basic thermophysical properties of the feedstock; however, due consideration of this issue has not been given due attention in the literature.

Let us further dwell in more detail on the studies devoted to determining, by computational and experimental methods, the main characteristics of feedstock and its components, including thermophysical characteristics.

In addition to various reference books on PIM technology [4, 16], the following widely cited studies [17-19] describe models for calculating feedstock thermophysical, mechanical, and rheological characteristics. These studies mainly present various analytical models for calculating the efficient characteristics of feedstocks as disperse-filled composites. The methods and results of the present investigation will present some of these models. In addition, Kate et al. [17-19] note that in addition to analytical models, which give too broad two-sided estimates for the effective thermal conductivity and mechanical properties, it is promising to calculate in software packages of multiscale multiphysics modeling, which use self-consistency and averaging methods. The disadvantage of numerical methods, in turn, is the necessity of a deterministic setting of the structure of a representative element of the feedstock volume, which is not always possible due to the complex shape of the dispersed filler and the complex structure of the polymer binder's blend. Therefore, combining analytical and numerical characterization methods with experimental ones is desirable to verify and eliminate the computational uncertainty associated with two-sided upper and lower estimates of physical characteristics.

Many investigations focus not only on methods for determining the characteristics of dispersed-filled composites but also quantitatively present the characteristics of feedstocks and their components. For example, some studies [20-22] describe the thermophysical properties of polyoxymethylene as one of the most essential types of binder for feedstocks. Weidenfeller et al. [23], Progelhof et al. [24], and Zhu et al. [25] describe the calculation methods and thermophysical properties of dispersed-filled composites, presenting, in particular, information on the thermophysical properties of polypropylene. Investigation [26] presents computational and experimental data on the thermophysical properties of feedstock based on polyoxymethylene and 42CrMo4 steel powder. Xu et al. [27], Mamunya et al. [28] and Markov [29] describe in detail the methods of calculating the thermophysical properties of dispersed-filled composites. In addition to describing the methods used, the study by Kowalski et al. [30] details the thermophysical properties of feedstock based on polyoxymethylene and 316L steel powder, and several studies [31-33] present information on the thermophysical properties of various waxes and paraffins.

In the field of additive technologies and injection molding of powders, new works are constantly published [33-36], devoted to various aspects of optimizing the materials used and production modes. However, there are relatively few new studies in the field of the thermophysical properties of processed materials. At the same time, thermophysics largely determines the process of injection molding of materials [37-39]. The literature presents an in-depth examination of the methods used to calculate and determine the thermophysical properties of feedstocks and the values of thermophysical characteristics of feedstocks and their components through experimental procedures. However, it does not present the results of a comparative analysis of the thermophysical properties of feedstocks with the same powder filler and the different most widely demanded types of binder based on polyoxymethylene and wax-polyolefin mixture. Thus, such a comparative analysis is an urgent task, and its results will allow technologists to make additional recommendations on one or another type of binder for producing various products.

3. Research Methods and Results

3.1. Composition and Structure of the Compared Powder-Polymer Mixtures

The objects of the current investigation are two industrial feedstocks with structural low-alloy steel powder as their base. The essential difference between these feedstocks is the type of polymer binder used: type 1 feedstock manufacturing uses a binder designed for solution-thermal debinding (i.e., using a wax-polyolefin mixture), whereas type 2 feedstock manufacturing uses a binder designed for catalytic debinding (i.e., using polyoxymethylene).

Both feedstocks have (61.9 ± 0.1) vol. % of 42CrMo4 steel powder in their bases with spherical particle sizes ranging from 2 to 16 μm with an average $D_{50} = 6 \mu\text{m}$. The binder for type 1 feedstock is a mixture of paraffin wax (PW), polypropylene (PP), and stearic acid (SA) in small amounts. The total volume of polypropylene is 38 % of the volume of the polymer blend, i.e., 14 % of the entire feedstock volume. In other words, the mass fraction of wax is 3.85 ± 0.05 % and that of polypropylene is 2.79 %. Polyoxymethylene (POM) is applied to the binder of the type 2 feedstock. Figure 1 shows the microstructure of the compared feedstocks as a result of scanning electron microscopy examination using the FEI Phenom ProX electron microscope.

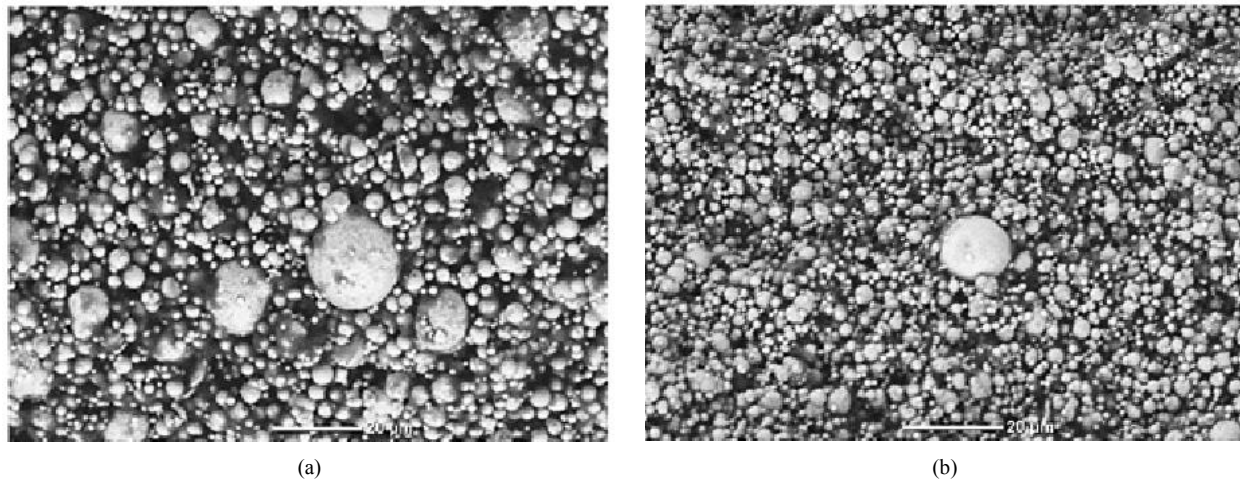


Figure 1. Microstructure of the compared feedstock types: (a) type 1 – with wax-polypropylene binder mixture; (b) type 2 – with polyoxymethylene

The obtained images (Figure 1) confirm that both feedstocks have a homogeneous microstructure and predominantly contain metallic particles of spherical shape, which ensures uniformity and reproducibility of shrinkage during sintering of part blanks.

Energy dispersive spectroscopy confirmed the chemical composition of 42CrMo4 steel powder on a brown sample (porous powder unsintered part with already removed the polymer binder). Figure 2 shows the microstructure of the investigated area of the brown material and the obtained energy dispersive spectrum. The energy dispersive spectra of 42CrMo4 steel powder in the compared feedstocks after binder removal were identical, indicating a qualitative and reproducible process of polymer removal.

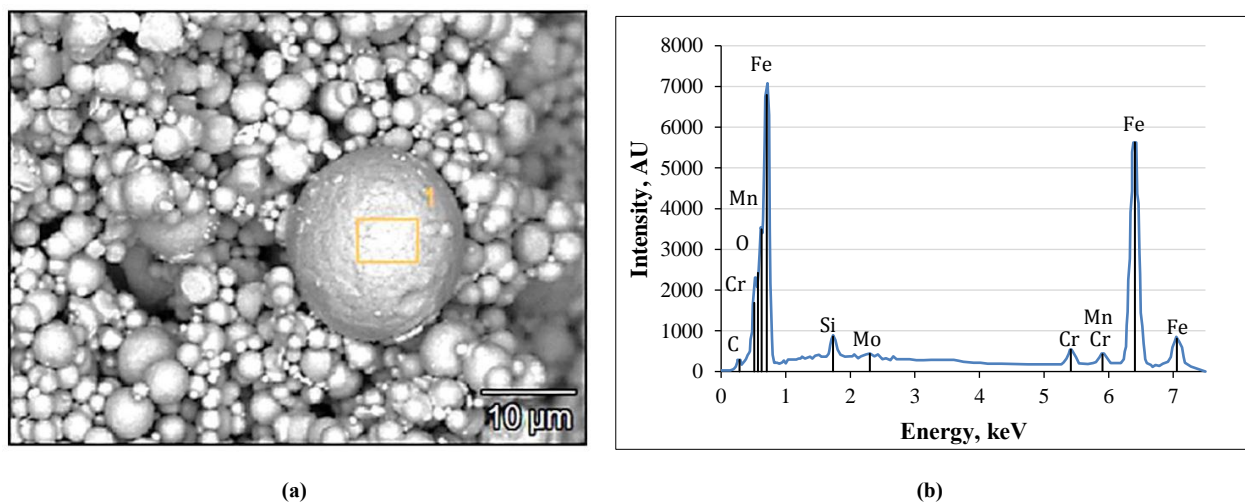


Figure 2. (a) Microstructures of the brown part; (b) energy dispersive spectrum, characterizing the chemical composition of the powder particles

3.2. Methods and Results of The Evaluation of Thermophysical Characteristics

The methodology and algorithm used in this study are presented as a flowchart in Figure 3.

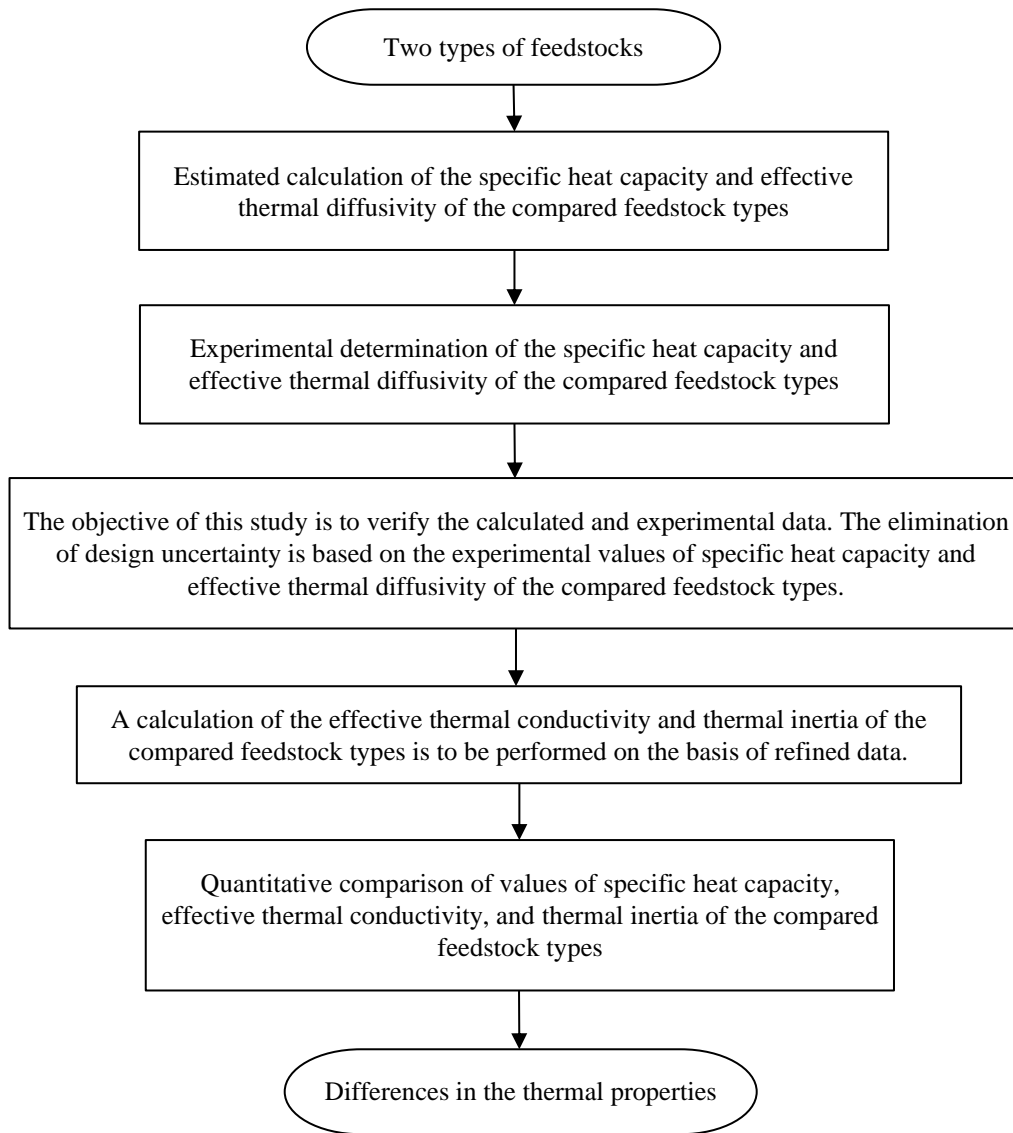


Figure 3. Flowchart describing the methodology and algorithm used in this research

The comparative investigation of polymer binder mixtures employed differential scanning calorimetry to elucidate the phase transition characteristics of the respective feedstocks. Measurements of specific heat flux used a Netzsch DSC 204F1 device with a heating rate $H_R = 10$ K/min in an inert argon atmosphere at a purge speed of the measuring cell of 50 ml/min according to ISO 11357-1:2009. Figure 4 shows the measured calorimetric curves.

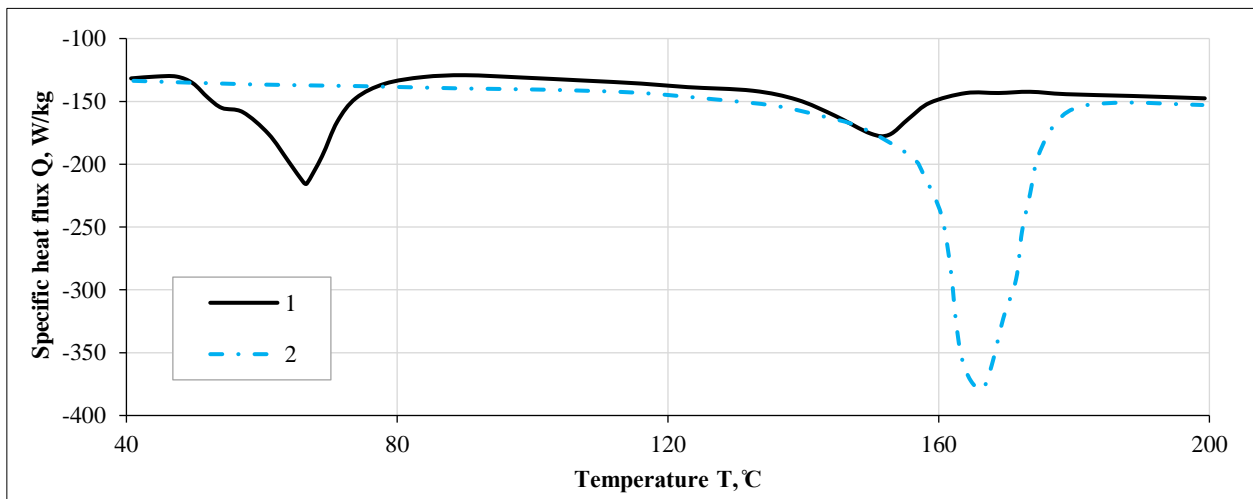


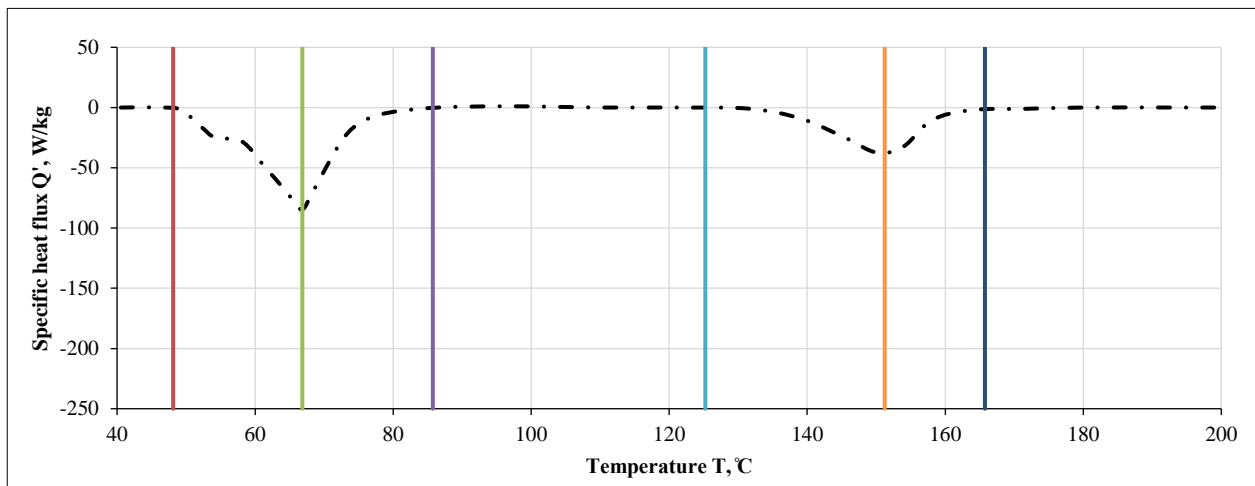
Figure 4. Calorimetric heating curves of feedstocks: 1 – type 1; 2 – type 2

The calorimetric curves $Q(T)$ presented in Figure 4 are transformable into temperature dependence of the specific heat flux $Q'(T)$, revealing information about the latent heat of the phase transition of the melting of polymer binder components in the studied feedstocks (Figure 5). Such transformation, introducing the zero reference for the heat of phase transition, simultaneously makes it possible to accurately determine the temperature of the beginning T_{M1} , maximum of intensity T_{M2} and temperature of the end of phase transition T_{M3} . It characterizes the temperature interval of the melting binder components and enables integration within the established limits according to expression (1), resulting in the determination of the specific heat of E_M melting phase transition for each component in the raw materials, considering the heating rate. It should be noted that the temperature values displayed in Table 1 are determined by the secant method according to ISO 11357-1:2009; the other temperature values are based on the derivative $d[Q'(T)]/dT$ value.

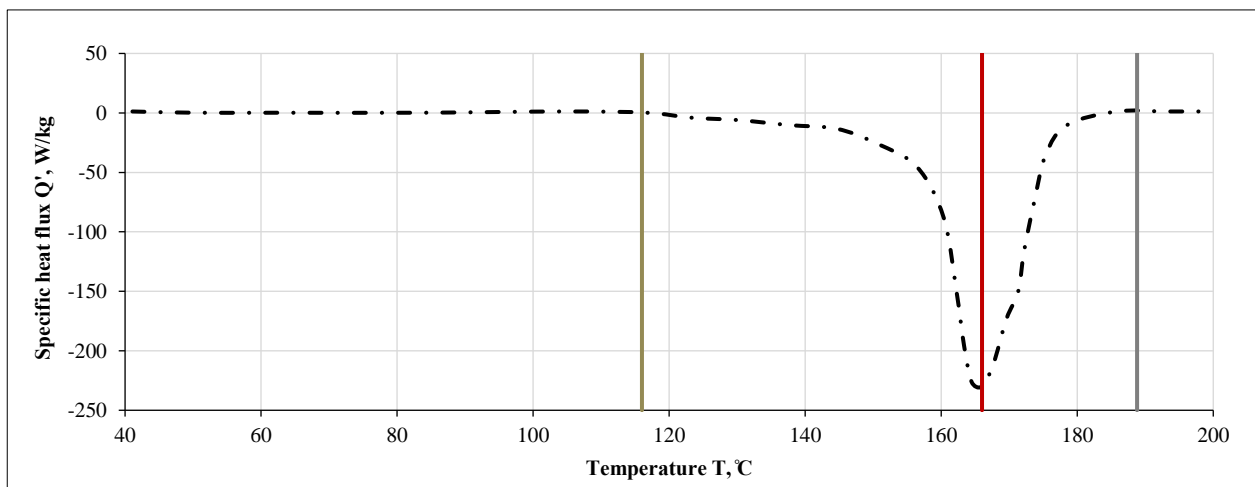
$$E_{Mi}^j = \int_{\frac{T_{M1_i}^j}{H_R}}^{\frac{T_{M3_i}^j}{H_R}} Q_i^j \left(\frac{T}{H_R} \right) d \frac{T}{H_R} \tag{1}$$

where E_{Mi}^j – specific heat of the melting phase transition of the j -th polymer component in the binder of the i -th feedstock; $T_{M3_i}^j$ and $T_{M1_i}^j$ – temperatures of the beginning and end of the melting phase transition of the j -th polymer component in the binder of the i -th feedstock; H_R – heating rate at calorimetric measurements; T – temperature; Q_i^j – specific heat flux from the phase transition of the j -th polymer component in the binder of the i -th feedstock.

The curves $Q'(T)$ shown in Figure 5 represent the temperature dependences of specific heat fluxes related only to the absorption of the latent energy of the melting phase transition of polymer binder components in the studied feedstocks, i.e., without considering the heat flux caused by changes in the heat capacity of the material and energy absorption during heating.



(a)



(b)

Figure 5. Temperature dependences of specific heat flux from the latent heat of melting phase transition of polymer binder components in the compared feedstocks: (a) for type 1 feedstock; (b) for type 2 feedstock

Table 1. Melting phase transition characteristics of the components of polymer binder blends in the compared feedstocks

Characteristic	The component type of feedstock polymer binder blend		
	Wax in type 1 feedstock	PP in type 1 feedstock	POM in type 2 feedstock
Melting point T_{M1} , °C	47 (59)	123 (139)	116 (161)
Temperature of maximum melting intensity T_{M2} , °C	66	151	166
Melting finish temperature T_{M3} , °C	(74) 86	(160) 166	(173) 188
Heat of melting E_M , kJ/kg	3.68	2.68	17.21

The calculation method for determining the specific heat capacity of dispersed-filled composites is most often based on the mixture rule, expressed as Equation 2-a. A series of studies revealed that the specific heat capacity values obtained for the feedstocks were artificially low; therefore, the authors of these studies used a modified mixture rule in the form of Equation 2-b supplemented with a correction factor for calculations [18-20]:

$$c_{pFi}(T) = c_{pPi}(T) \cdot X_{Pi} + c_{pBi}(T) \cdot X_{Bi} \quad (2-a)$$

$$c_{pFi}(T) = c_{pPi}(T) \cdot X_{Pi} + c_{pBi}(T) \cdot X_{Bi} \quad (2-b)$$

where c_{pFi} – specific heat capacity of the i -th feedstock; c_{pPi} – specific heat capacity of the metal powder in the i -th feedstock; c_{pBi} – specific heat capacity of the polymer binder in the i -th feedstock; X_{Pi} – mass fraction of the metal powder in i -th feedstock; X_{Bi} – mass fraction of the binder in i -th feedstock; A_0 – correction factor equal to 0.2 [4].

Calculations using Equation 2-b require a transition from the volume to mass fractions of the metal powder and polymer binder in the feedstock performed by calculation according to Equation 3:

$$X_{Pi} = \frac{\varphi_{Pi} \cdot \rho_{Pi}}{\varphi_{Pi} \cdot \rho_{Pi} + \varphi_{Bi} \cdot \rho_{Bi}} \quad (3)$$

$$X_{Bi} = 1 - X_{Pi}$$

Calculations took the following values: $\rho_{Pi} = 7810 \text{ kg/m}^3$ – density of steel 42CrMo4; ρ_{Bi} – density of binder in i -th feedstock, which in case of type 2 feedstock with binder on the basis of polyoxymethylene is equal to $\rho_{Bi} = 1415 \text{ kg/m}^3$, and in case of type 1 feedstock with binder in the form of a mixture of wax and polypropylene is equal to $\rho_{Bi} = 884 \text{ kg/m}^3$. Temperature changes in density were neglected in the calculations. Calculating the specific heat capacities of feedstocks according to Equation (2-b) involves the characteristics of the metal powder and polymer binder. Equation 4 describes a well-known temperature dependence of the specific heat capacity of 42CrMo4 steel with a linear correlation coefficient $r = 0.994$ in the temperature range from 0 to 800 °C:

$$c_{pp}(T) = 445\,125 + 0,286 \cdot T \quad (4)$$

The temperature-dependent specific heat capacities of the polymer components also require description. Calculating the specific heat capacities of feedstocks using Equation (2-b) involved the necessary dependencies built on [21-23] and defined further for each component of polymer mixtures as an approximation 5:

$$\begin{aligned} c_p^{PP}(T) &= 1821,58 + 5,40 \cdot T, r = 0,988; \\ c_p^{WAX}(T) &= 2182,78 + 2,93 \cdot T, r = 0,999; \\ c_p^{POW}(T) &= 1365,87 + 1,52 \cdot T, r = 0,871. \end{aligned} \quad (5)$$

Thus, at 20 °C, the heat capacity of wax will be 2240 J/(kg·K); polypropylene – 1930 J/(kg·K); polyoxymethylene – 1400 J/(kg·K).

For the compared feedstocks, to evaluate the accuracy of the approximate calculation models, we further compared the calculated values of specific heat capacities with the obtained experimental temperature dependence. The comparison involved calculating the relative discrepancy between the values obtained experimentally and computationally. The results confirmed that model (2b) is the most reliable selection when using computational methods. Figure 6 shows the temperature dependence of the specific heat capacities of the raw materials. The dependences were calculated according to model (2b) and obtained experimentally.

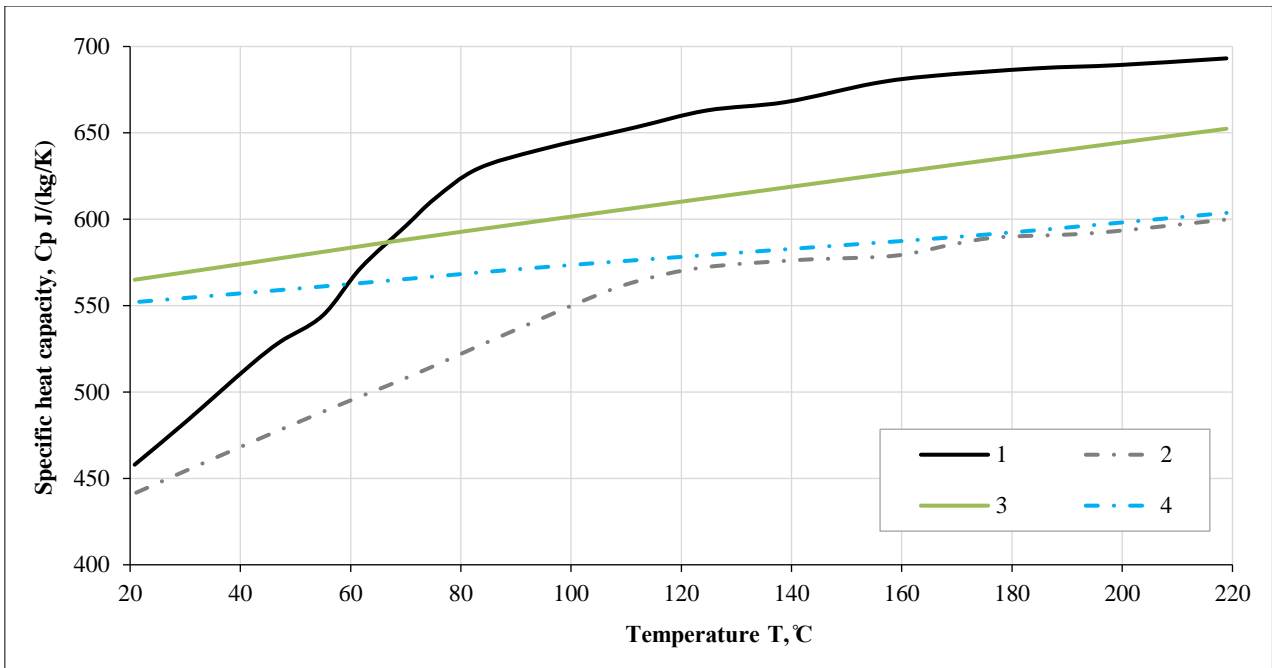


Figure 6. Temperature dependence of specific heat capacity of the compared feedstocks: 1 – experimental data for type 1 feedstock, 2 – experimental data for type 2 feedstock, 3 – calculated data for type 1 feedstock, 4 – calculated data for type 2 feedstock.

Figure 6 shows that in the area of feedstock processing temperatures, the relative discrepancy (relative difference) between the calculated and experimental values of specific heat capacity for both feedstocks does not exceed 10 %. Thus, the values of the specific heat capacity of feedstocks calculated on the basis of model (2b) have acceptable accuracy; accordingly, the obtained experimental temperature dependence of the specific heat capacity for each of the feedstocks are correct and, therefore, can be applied in the future for modeling casting processes using appropriate software.

Since for each feedstock, the established calculated temperature dependence of specific heat capacity and the obtained experimental values are accurate enough, it becomes possible to correctly compare the specific heat capacities of type 1 and type 2 feedstocks according to experimental data and calculated estimation models (Figure 7). As a result, in a wide range of temperatures, the specific heat capacity of type 1 feedstock (with wax-polyolefin mixture binder) is superior to type 2 feedstock (with polyoxymethylene binder), and the difference in heat capacity reaches 6 % according to the calculated data and 16 % according to the experimental data.

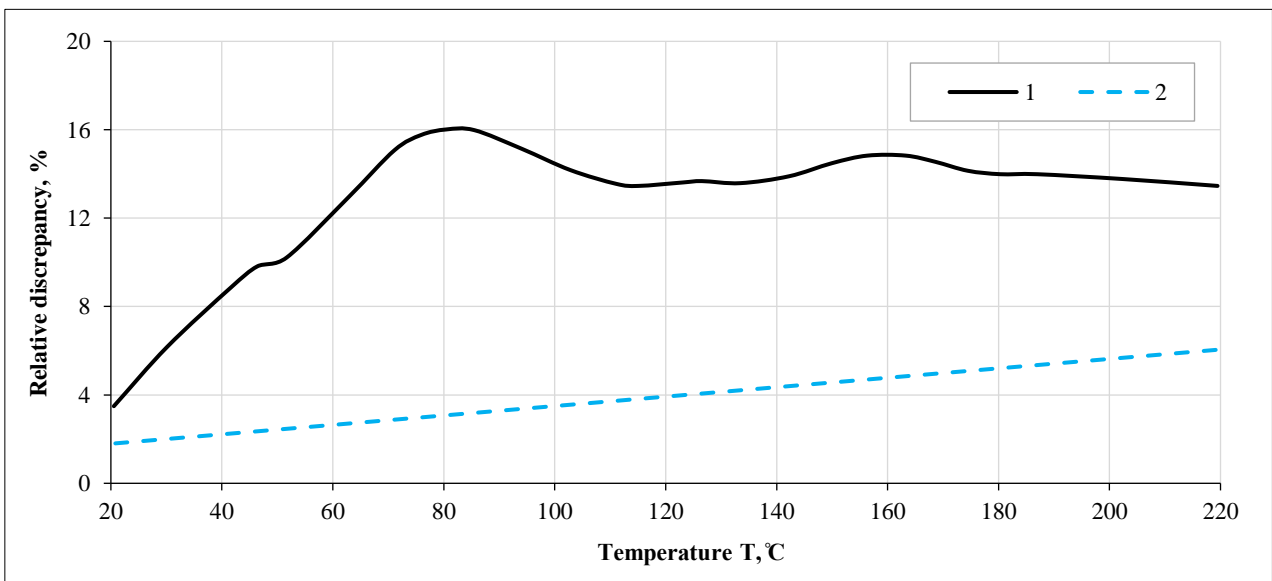


Figure 7. Temperature dependences of specific heat capacity of the compared feedstocks: 1 – experimental data for type 1 feedstock, 2 – experimental data for type 2 feedstock, 3 – calculated data for type 1 feedstock, 4 – calculated data for type 2 feedstock.

The temperature dependences of the specific heat capacity of feedstocks $c_{PF}(T)$ and specific heat flux $Q'(T)$ due to the melting phase transition of polymer binder components in feedstocks obtained based on calorimetric curves make it possible to use Equation 6 to estimate the minimum work required for thermal plasticization of 1 kg of feedstock. This work summarizes the energy input for melting and heating to a given temperature T . Figure 8 graphically shows the calculation results for each type of feedstock.

$$W_{PLi} = \int_T c_{PFi}(T)dT + \int_{\frac{T}{HR}} Q'_i \left(\frac{T}{HR}\right) d\frac{T}{HR} \tag{6}$$

where W_{PLi} is work required for thermal plasticization of 1 kg of feedstock

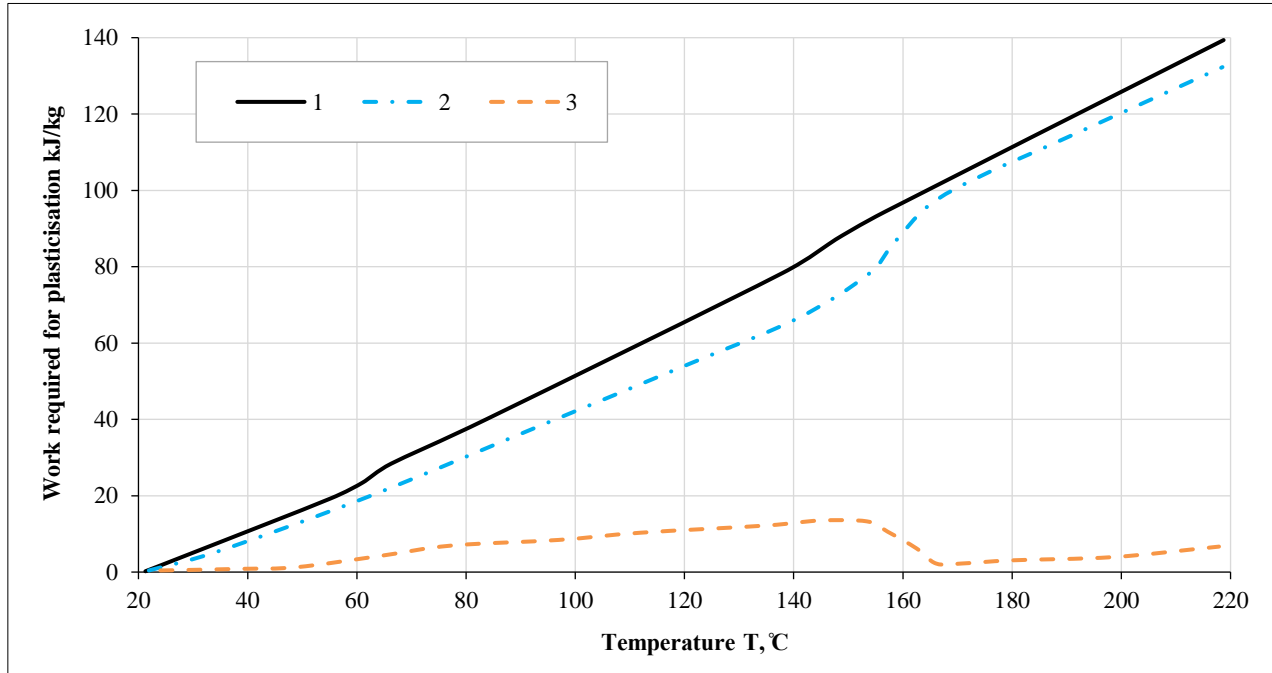


Figure 8. Work spent on melting and heating 1 kg of feedstock from $T = 20\text{ }^\circ\text{C}$ to a given temperature T : 1 – for the type 1 feedstock; 2 – for the type 2 feedstock; 3 – difference for the compared feedstock types

The dependencies in Figure 8 show that in the investigated temperature range, they can be linearized; i.e., for the estimated calculations of the heat energy released in the green part when its temperature changes, it is possible to use an equation of the form $\Delta Q = \bar{c} \cdot \Delta T$, where \bar{c} – the apparent heat capacity of the material. With a linear correlation coefficient $r = 0.999$, the value for type 1 feedstock is 685.66 kJ/(kg·K), and for type 2 – 674.35 kJ/(kg·K) at $r = 0.992$.

The thermal conductivity of feedstocks also significantly influences the choice of technological parameters employed in the casting process of MIM feedstocks, particularly in the filling of the molding cavity and in the breathing of the molded parts. In this context, further investigation was undertaken into the thermal conductivity of the compared feedstocks. Thermal conductivity of composite materials is a structurally sensitive physical quantity for which quantitative evaluation techniques based on different modeling concepts have been developed [26]. It is crucial to be able to quantitatively define the lower and upper estimates of the effective thermal conductivity of representative elements within composite or blended material volumes. As is well-established, the range of potential effective thermal conductivity values associated with such two-sided estimates is typically vast [27]. Therefore, it is of great importance to exercise caution when selecting the computational models and to ensure the accuracy of the thermophysical characteristics of the composite or blended material components, which serve as the initial data for the calculation [28-30].

In the present work, to calculate the effective thermal conductivity of the compared feedstocks, we set the temperature dependences of the thermal conductivity of the components of the polymer binders of the feedstocks: polyoxymethylene, polypropylene, and wax. The thermal conductivity of polymer components was approximately given based on the data presented in [26, 30-32] and actual values of phase transition temperatures of binder components in feedstocks determined in the present work (Table 1). Figure 9 shows the graphs of the temperature dependences of the heat conductivity of the polymer binder components of feedstocks [32, 40, 41].

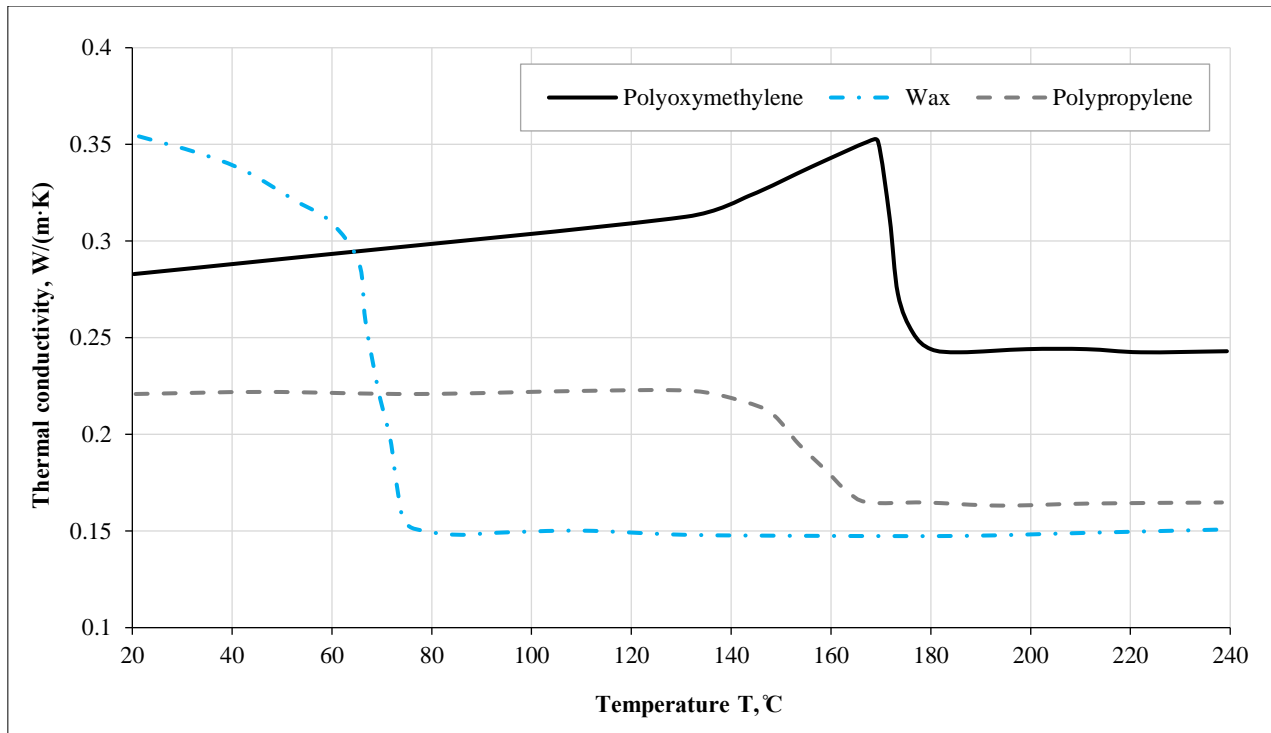


Figure 9. Thermal conductivities of the components of polymer binder blends

Since the type 1 feedstock binder is a polymer blend whose structure and properties change with temperature, the effective thermal conductivity of this blend was calculated.

When calculating the effective thermal conductivity of emulsions, the mixture rule in Equation 7-a is only a very rough approximation corresponding to the equivalent model in the form of plates parallel to the heat flux [26]. A more accurate calculation of the effective thermal conductivity of emulsions can use the dependence for calculating that of a polymer binder blend, which is in the state of a freely dispersed emulsion at high temperatures (Equation 7-b):

$$\lambda_B^{EF}(T) = \lambda_W(T) \cdot X_W + \lambda_{PP}(T) \cdot X_{PP} \tag{7-a}$$

$$\lambda_B^{EF}(T) = \lambda_W(T) \cdot X_W + \lambda_{PP}(T) \cdot X_{PP} - A_1 \cdot X_W \cdot X_{PP} \cdot |\lambda_W(T) - \lambda_{PP}(T)| \tag{7-b}$$

where λ_B^{EF} – effective thermal conductivity of the polymer binder blend; λ_W – wax thermal conductivity; λ_{PP} – polypropylene thermal conductivity; X_W – mass fraction of wax in the polymer binder composition; X_{PP} – mass fraction of wax in the composition of the polymer binder; A_1 – coefficient taking the value from 0.53 to 0.72.

A model in the form of Equation 8 is proposed for a binder with a structure in the form of interpenetrating solid polymer phases:

$$\lambda_B^{EF}(T) = \lambda_W(T) \cdot \left[\Omega^2 + \frac{\lambda_W(T) \cdot (1-\Omega)^2}{\lambda_{PP}(T)} + \frac{2 \cdot \lambda_W(T) \cdot \Omega \cdot (1-\Omega)}{\lambda_{PP}(T) + \lambda_{PP}(T) \cdot \Omega \cdot \left(\frac{\lambda_W(T)}{\lambda_{PP}(T)} - 1 \right)} \right] \tag{8}$$

$$\Omega = 0,5 - \cos\left(\frac{\arccos(2 \cdot \varphi_{PP}^B - 1)}{3}\right)$$

where φ_{PP}^B – volume fraction of polypropylene in the composition of the type 1 binder mixture.

Figure 10 shows the temperature dependence of the effective thermal conductivity of the feedstock type 1 polymer binder blend calculated according to models (7a, 7b) and (8). The mixture rule (7a) gives overestimated results for all calculated temperatures (curve 1). The dependences of effective thermal conductivity obtained according to model (7b) for freely dispersed emulsions (curve 3) and model (8) for a coherently dispersed system of interpenetrating solid phases (curve 2) practically coincide, except for the temperature region at which the polymer mixture is in the suspension state. For further calculations, the effective thermal conductivity of the polymer mixture was taken as the average (curve 4) of the values obtained from models (7b) and (8).

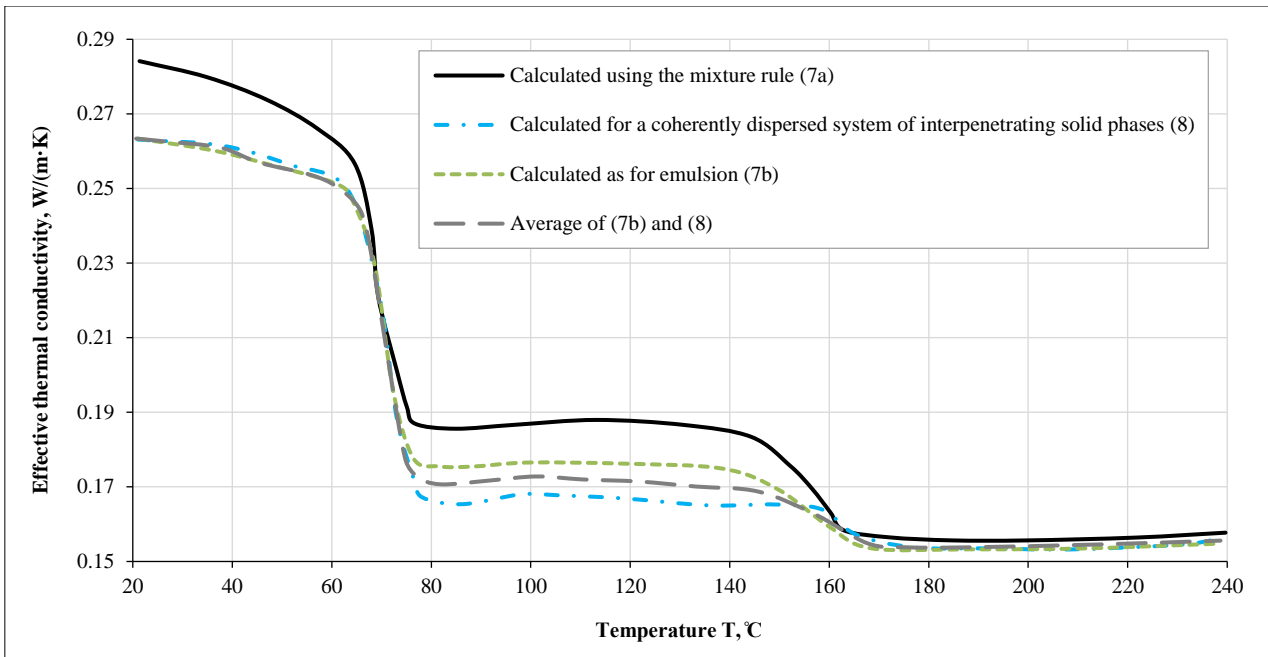


Figure 10. Temperature dependence of effective thermal conductivity of the wax-polyolefin binder of type 1 feedstock

The presented calculations make it possible to compare the effective thermal conductivities of type 1 and type 2 polymer feedstock binders. Such a comparison in Figure 11 shows that in the range of processing temperatures, the thermal conductivity of type 2 feedstock binder (with polyoxymethylene) exceeds that of type 1 feedstock binder by 1.5-2.0 times.

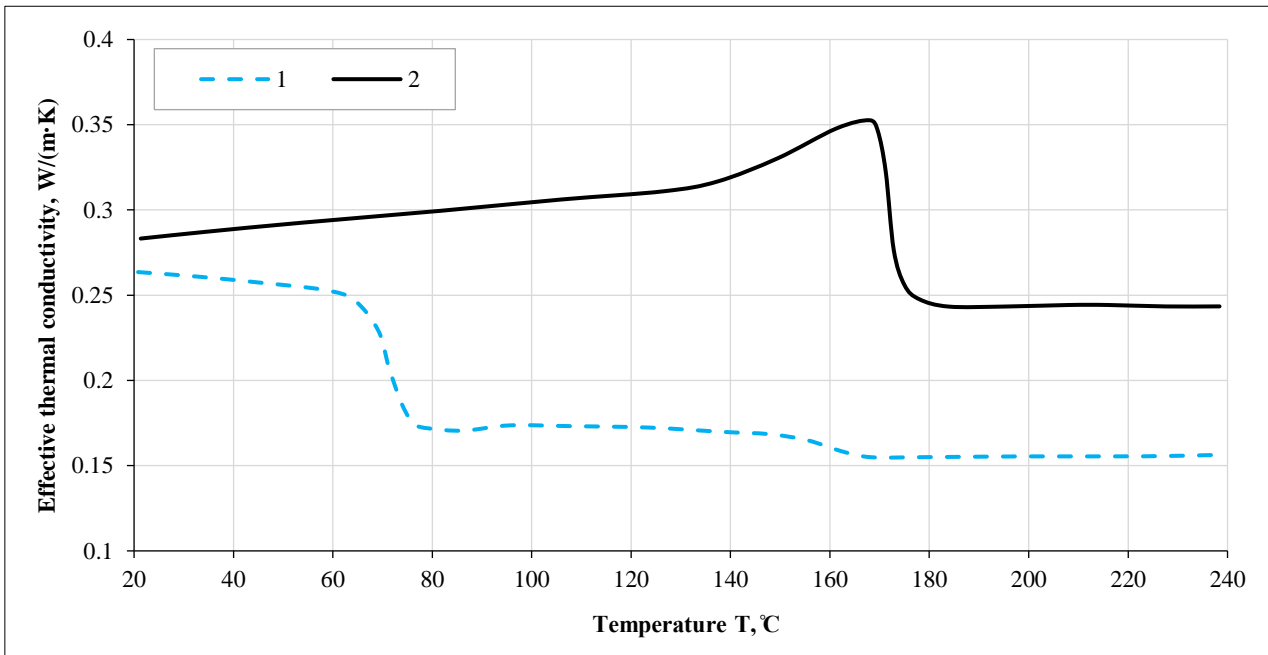


Figure 11. Effective thermal conductivity of polymer binder in feedstocks: 1 – in type 1 feedstock; 2 – in type 2 feedstock

Calculations of the effective thermal conductivity of the investigated feedstocks involved the temperature dependence of the thermal conductivity of 42CrMo4 steel. Equation 9 describes this dependence with a correlation coefficient $r = 0.998$ in the temperature range from 0 °C to 250 °C.

$$\lambda_p(T) = 32\,361 + 0.028 \cdot T \tag{9}$$

where λ_p – the thermal conductivity of steel powder filler of feedstocks.

Various models can be used to calculate the effective thermal conductivity of feedstocks [26]. The Maxwell model in the form of Equation 10 or the Rayleigh model in the form of Equation 11 applies for the "lower" estimation of feedstock thermal conductivity:

$$\lambda_F^{EF}(T) = \lambda_P(T) \frac{\lambda_B^{EF}(T) + 2 \cdot \lambda_P(T) + 2 \cdot \varphi_P \cdot (\lambda_B^{EF}(T) - \lambda_P(T))}{\lambda_B^{EF}(T) + 2 \cdot \lambda_P(T) - \varphi_P \cdot (\lambda_B^{EF}(T) - \lambda_P(T))} \tag{10}$$

$$\lambda_F^{EF}(T) = \lambda_B^{EF}(T) \cdot \left[1 + \frac{3 \cdot \varphi_P}{\left(\frac{\lambda_P(T) - 2 \cdot \lambda_B^{EF}(T)}{\lambda_P(T) - \lambda_B^{EF}(T)} \right) - \varphi_P + 1,569 \cdot \left(\frac{\lambda_P(T) - \lambda_B^{EF}(T)}{3 \cdot \lambda_P(T) - 4 \cdot \lambda_B^{EF}(T)} \right)} \right] \tag{11}$$

where λ_F^{EF} – feedstock effective thermal conductivity.

The Lichtenecker & Ratcliffe model in the form of Equation 12 or the Lewis & Nielsen model in the form of Equation 13 applies to the "upper" estimate of the feedstock effective thermal conductivity, as shown in Figure 12.

$$\lambda_F^{EF}(T) = \lambda_P(T)^{\varphi_P} \cdot \lambda_B^{EF}(T)^{(1-\varphi_P)} \tag{12}$$

$$\lambda_F^{EF}(T) = \lambda_B^{EF}(T) \cdot \left[\frac{1 + \varphi_P \cdot A_2 \cdot \vartheta(T)}{1 - \varphi_P \cdot \Phi \cdot \vartheta(T)} \right], \vartheta(T) = \left(\frac{\lambda_P(T)}{\lambda_B^{EF}(T)} - 1 \right) \cdot \left(\frac{\lambda_P(T)}{\lambda_B^{EF}(T)} + A_2 \right), \Phi = 1 + \varphi_P \cdot \left(\frac{1 - \varphi_P^{MAX}}{(\varphi_P^{MAX})^2} \right) \tag{13}$$

The Lewis-Nielsen model is notable for its consideration of percolation, whereby the actual volume filling is compared with the maximum possible volume based on the filler particle shape factor. In the calculations, the coefficient A_2 of the spherical particle shape factor was 1.5; the coefficient φ_P^{MAX} , responsible for the proximity to the limit filling, was 0.65 [26].

The Lewis-Nielsen model is notable for its consideration of percolation, whereby the actual volume filling is compared with the maximum possible volume based on the filler particle shape factor. In the calculations, the coefficient A_2 of the spherical particle shape factor was 1.5; the coefficient responsible for the proximity to the limit filling was 0.65 [26].

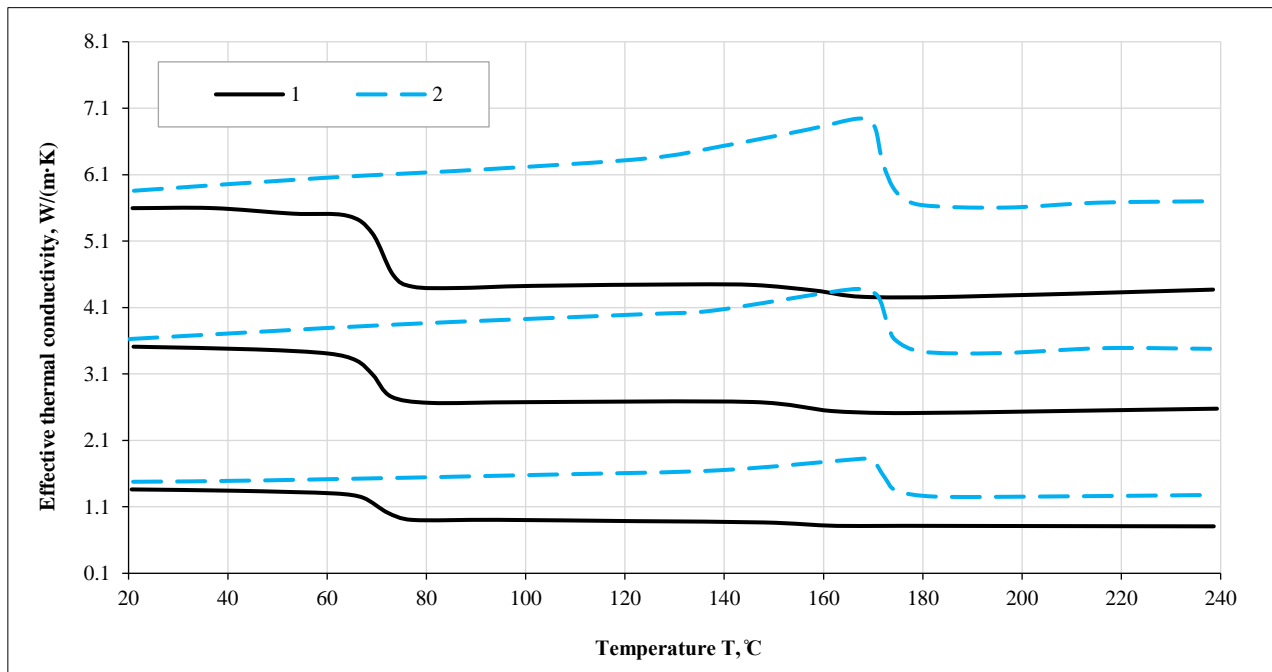


Figure 12. Two-sided estimates and average value of effective thermal conductivity of feedstocks of the compared types: 1 – type 1; 2 – type 2

Comparing the kinetics of thermal processes in the casting materials of the studied feedstocks involved calculating the thermal diffusivity and thermal inertia of each feedstock. Equation 14 is used for the calculation of the effective thermal diffusivity, and the value of the thermal inertia of the feedstock is calculated using Equation 15. In the academic literature on the subject of heat transfer between the casting and the mold, the aforementioned thermophysical characteristic is frequently referred to as either the heat storage capacity of the material or the heat storage coefficient.

$$\chi_F^{EF}{}_i(T) = \frac{\lambda_F^{EF}{}_i(T)}{\rho_{Fi} \cdot c_{pFi}(T)} \tag{14}$$

$$I_F^{EF}{}_i(T) = \sqrt{\rho_{Fi} \cdot c_{pFi}(T) \cdot \lambda_F^{EF}{}_i(T)} \tag{15}$$

where $\chi_F^{EF}{}_i$ – effective thermal diffusivity of the i -th feedstock material; $I_F^{EF}{}_i$ – thermal inertia of the i -th feedstock; ρ_{Fi} – density of the i -th feedstock.

Figure 13 presents the calculated two-sided estimates and average values of the thermal inertia and effective thermal diffusivity of the feedstocks. The densities of feedstocks were assumed constant in the calculation: $\rho_{F1} = 5.1269 \pm 0.0913 \text{ g/cm}^3$; $\rho_{F2} = 5.3671 \pm 0.0852 \text{ g/cm}^3$. The values of solid feedstock densities were obtained by the pycnometric method according to ISO 12154:2014 using a G-DenPyc 2900 helium pycnometer with a limit of relative instrumental error of $\pm 0.02 \%$.

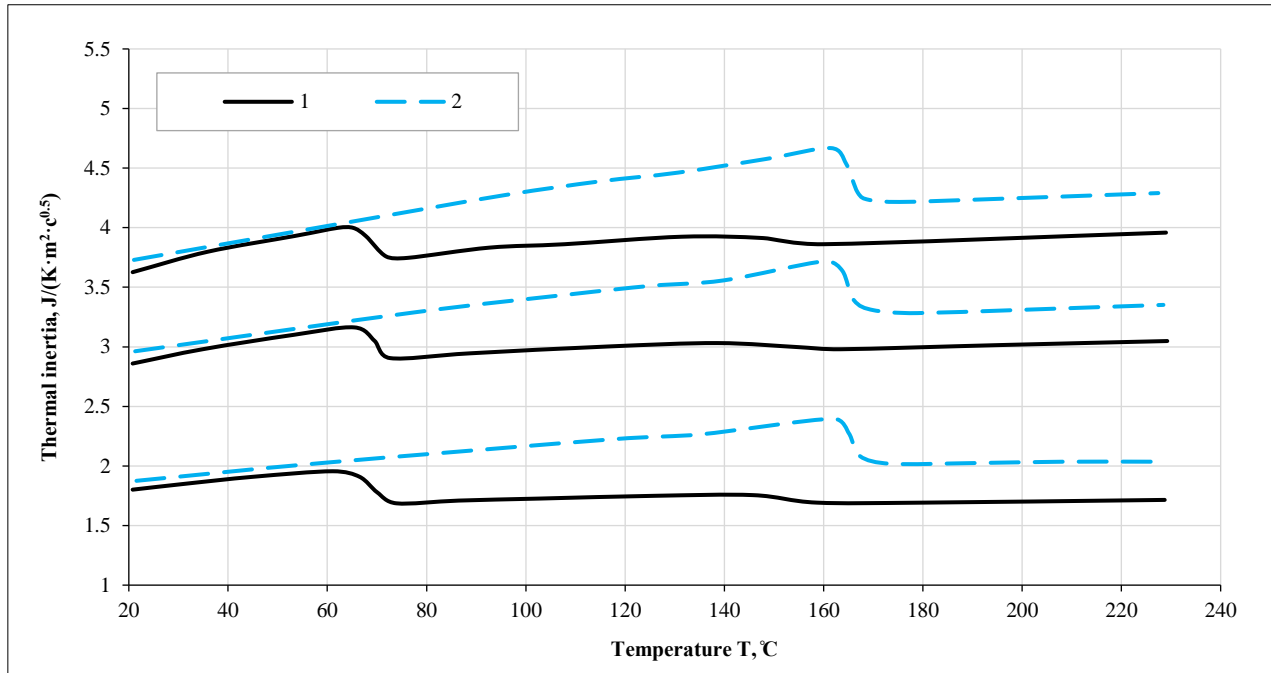
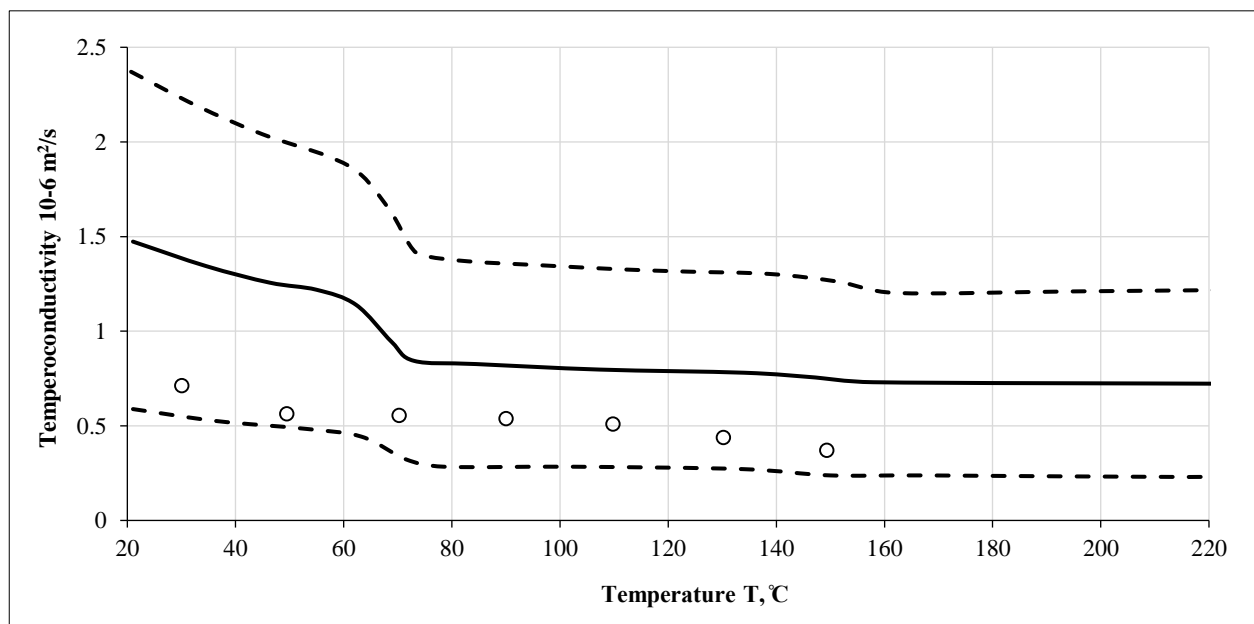


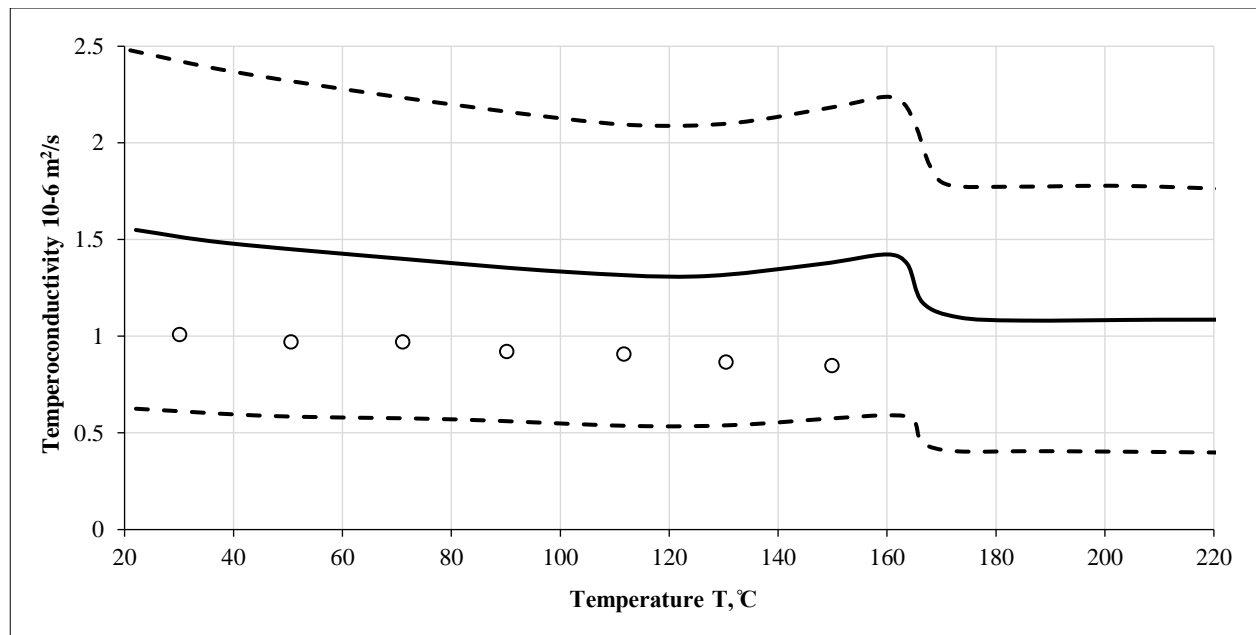
Figure 13. Two-sided estimates and average value of thermal inertia: 1 – type 1 feedstock; 2 – type 2 feedstock

The correctness assessment of the calculated values of the feedstock diffusivity involved verification with experimental data measured according to ASTM E1461 by the laser flash method (LFA) on the Netzsch LFA427 device with a limit of diffusivity measurement error of $\pm 2\%$. Samples in the form of a disk with a diameter of 12.5 mm and a thickness of 1.5 mm were used for measurements.

As a result of verification of the calculated and experimental values of the thermal diffusivities of both feedstocks (Figure 14), we can conclude that the measured experimental values are within the two-sided analytical estimates, and the average calculated value coincides with the experimental data with satisfactory accuracy. Measurements occurred at different temperatures up to plasticization of the samples. Note that for both feedstocks, the upper calculated estimates of thermal diffusivity significantly exceed the experimental values. It is important to underline that this ratio may vary significantly during the flow and breathing stages, when the percolation mechanisms of heat transfer between the highly conductive particles of the filler material begin to operate.



(a)



(b)

Figure 14. Experimental data, calculated two-sided estimates, and average thermal diffusivity of the compared feedstocks: (a) type 1 feedstock; (b) type 2 feedstock

The obtained analytical dependences of thermal diffusivity, thermal conductivity, and thermal inertia for both feedstocks are correct (adequate) and applicable in the modeling of casting processes using specialized software.

4. Analysis and Discussion of the Results

Investigation of feedstocks of two types produced using fundamentally different types of polymer binder blends and 42CrMo4 steel powder yielded a general characterization of their thermophysical properties. The investigation was conducted using both computational and experimental methods. The results of the analysis demonstrate a satisfactory correlation between the calculated and experimental data sets. In addition, the experimental data obtained made it possible to eliminate the calculated uncertainty.

Figure 8 shows that the melting and heating of feedstock to the same temperature T in the case of type 1 feedstock requires 5-15% more energy than for type 2 feedstock, i.e., at the same temperature, the wax-polyolefin binder feedstock stores more thermal energy than the polyoxymethylene-based feedstock. At the same casting modes in the same molds, this circumstance should shift the moment of the beginning of solidification and will lead to a difference in the solidification rate of green parts (castings) from the studied feedstocks. Accordingly, it should lead to the necessity of using different breathing modes at the final stage of casting parts from these feedstocks.

The specific heat capacity of the studied feedstocks is 1.2-1.4 times higher than that of steel but 3.1-5.6 times lower than that of polymers used as binders in feedstocks. The relatively low heat capacity of the slurry at casting into cold molds threatens premature disconnection of the material solidification in the molding cavity from the extruder working cylinder feeding at "freezing" of the thin section of the channels of the feed system even before complete solidification of the molded part, resulting in the inevitable occurrence of a shrinkage cavity in the casting. The difference in the thermophysical properties of polymers and MIM feedstocks leads to the impossibility of using the norms of casting technological modes used in the plastic industry.

In addition, the obtained quantitative estimates made it possible to compare the effective thermal conductivity of feedstocks. At temperatures ranging from 80 to 210 °C, the thermal conductivity of type 2 feedstock (with polyoxymethylene) is approximately 1.3-1.8 times higher than that of feedstock with wax-polyolefin binder. The difference in the thermophysical properties of the compared feedstock types is due to the different properties of the used polymer binders. However, if the difference in specific heat capacities of the studied feedstocks is less than 15 %, the difference in effective thermal conductivities at processing temperatures is 40-70%. This should lead to essentially different kinetics of nonequilibrium thermal processes when filling the mold cavity and breathing molded products from these feedstocks.

The obtained dependences made it possible to quantitatively compare the kinetics of thermal processes in the material of green parts during their molding from the studied feedstocks. Under nonequilibrium casting conditions, the rate of temperature field equalization in type 2 feedstock (with polyoxymethylene) is higher than that in type 1 feedstock with

wax-polyolefin binder. At temperatures from 80 °C to 220 °C, which corresponds to the processing temperatures, the difference in thermal conductivity is vast and reaches 1.5-2 times. However, in the same temperature range, type 2 feedstock has 1.1-1.3 times higher thermal inertia, which means that the kinetic effects of thermal processes during casting are less significant for this material.

The presented results for the compared feedstock types have some applicability limitations: they are correct for various steel powder fillers and qualitatively correct for other metals. However, for feedstock fillers with significantly different thermophysical properties (such as some ceramics), such calculations need to be repeated, which may become a direction for further research.

If we compare the present results with those of previously published works, we can highlight the following features. Unlike previous studies [17-19, 26, 30], this article is not aimed at describing computational methods or at determining the thermophysical characteristics of a specific feedstock for using these data to model casting processes. In this work, for the first time, the thermophysical properties of feedstocks with two fundamentally different types of polymer binders were compared, which made it possible to identify their advantages and disadvantages. In addition, it was previously noted in [26, 30] that methods for calculating the thermophysical characteristics of feedstock provide too broad two-sided estimates and, to eliminate this calculated uncertainty, they should be supplemented with an experimental determination of thermal diffusivity. However, in contrast to previous studies [26, 30], in this research, after updating the thermal conductivity for feedstocks using experimental data, their thermal inertia was calculated for the first time. This made it possible to compare the kinetics of thermal processes during the formation of the studied feedstocks and draw appropriate conclusions. The approach proposed in this study for assessing thermal inertia can be used when comparing the molding features of other feedstocks with various combinations of powder filler and polymer binder.

5. Conclusion

The research results showed that feedstocks based on the polymer binder blend for catalytic debinding are more technological in their thermophysical properties than feedstocks with polymer binder blends for solution-thermal debinding: kinetic effects in thermal processes during the processing of feedstock based on polyoxymethylene are less significant, which facilitates moldability. The rate of temperature field equalization in the feedstock based on polyoxymethylene is significantly higher; accordingly, the spatial gradient of the temperature field in the casting should be less than that in the casting from the feedstock with wax-polyolefin binder, which should lead to a more uniform field of deformations during material shrinkage. The technological advantages of wax-polyolefin-bonded feedstock include processing at lower temperatures than those of polyoxymethylene-based feedstock.

The difference in the polymer binder compositions leads to different thermophysical characteristics of the feedstocks, which entails determining the parameters of the technological modes of processing each feedstock into a product. The specific heat capacity of the studied feedstocks is insignificantly higher than steel but 3.1-5.6 times lower than that of the polymer binders in the feedstocks. Thus, the effective thermal conductivity of MIM feedstocks is approximately 15-30 times lower than steel but 5-20 times higher than that of polymers. The relatively low heat capacity and simultaneously relatively high thermal conductivity of MIM feedstock compared with unfilled polymers do not make it possible to use the technological modes and tooling used in casting polymers due to the increased cooling rate of the molded feedstock when using a cold-channel feed system. This investigation has shown for the first time that powder-polymer mixtures with a binder of solution-thermal debinding are preferable for molding semi-finished products with relatively large-sized elements with a risk of shrinkage defects. Powder-polymer mixtures with a binder for catalytic debinding are expedient for molding composite semi-finished products with thin-walled geometric elements.

6. Declarations

6.1. Author Contributions

Conceptualization, A.N.M. and M.S.M.; methodology, A.N.M.; software, M.S.M.; validation, A.N.M. and M.S.M.; formal analysis, M.A.K.; investigation, M.S.M. and M.A.K.; resources, A.N.M.; data curation, M.A.K. and M.S.M.; writing—original draft preparation, M.A.K.; writing—review and editing, M.A.K.; visualization, M.A.K.; supervision, A.N.M.; project administration, A.N.M. and M.S.M.; funding acquisition, A.N.M. All authors have read and agreed to the published version of the manuscript.

6.2. Data Availability Statement

The data presented in this study are available in the article.

6.3. Funding

The study was supported by a grant from the Russian Science Foundation № 23-79-10258, <https://rscf.ru/en/project/23-79-10258/>.

6.4. Conflicts of Interest

The authors declare no conflict of interest.

7. References

- [1] Gonzalez-Gutierrez, J., Beulke, G., & Emri, I. (2012). Powder Injection Molding of Metal and Ceramic Parts. Some Critical Issues for Injection Molding. IntechOpen, London, United Kingdom. doi:10.5772/38070.
- [2] Currie, E. P. K., Norde, W., & Cohen Stuart, M. A. (2003). Tethered polymer chains: surface chemistry and their impact on colloidal and surface properties. *Advances in Colloid and Interface Science*, 100–102, 205–265. doi:10.1016/s0001-8686(02)00061-1.
- [3] Kutsbakh, A. A., Muranov, A. N., Semenov, A. B., & Semenov, B. I. (2019). Outstanding problems of numerical simulation of the process of injection molding of PIM-feedstocks and component quality. *IOP Conference Series: Materials Science and Engineering*, 525, 012031. doi:10.1088/1757-899x/525/1/012031.
- [4] Heaney, D. F. (2012). Designing for Metal Injection Molding (MIM). *Handbook of Metal Injection Molding*, 29–49. doi:10.1533/9780857096234.1.29.
- [5] Semenov, A. B., Kutsbakh, A. A., Muranov, A. N., & Semenov, B. I. (2019). Metallurgy of thixotropic materials: The experience of organizing the processing of structural materials in engineering Thixo and MIM methods. *IOP Conference Series: Materials Science and Engineering*, 683(1), 12056. doi:10.1088/1757-899X/683/1/012056.
- [6] Urtekin, L., Yılan, F., & Şahin, İ. B. (2023). Optimization of Rheology Parameters for Feedstock by Powder Injection Molding (PIM) Via Taguchi Analysis. *International Journal of Integrated Engineering*, 15(7), 89–101. doi:10.30880/IJIE.2023.15.07.009.
- [7] Haghniaz, F., Delbergue, D., Côté, R., & Demers, V. (2023). Mold filling behaviour of LPIM feedstocks using numerical simulations and real-scale injections. *Powder Metallurgy*, 66(5), 436–449. doi:10.1080/00325899.2023.2218678.
- [8] Nguyen, T. K., & Pham, A. D. (2023). An Investigation on Pressure-Specific Volume–Temperature Behaviors of a Thermoplastic Under Industrial Conditions Using a Hot Runner Manifold. *International Journal of Precision Engineering and Manufacturing*, 24(10), 1845–1853. doi:10.1007/s12541-023-00847-y.
- [9] Muranov, A. N., Semenov, A. B., Kutsbakh, A. A., & Semenov, B. I. (2020). Specific Volume and Features of Compaction in Molding of Powder–Polymer Mixtures with Wax–Polypropylene Binder. *Polymer Science - Series D*, 13(2), 228–234. doi:10.1134/S1995421220020173.
- [10] Kostin, D. V., Parkhomenko, A. V., Amosov, A. P., Samboruk, A. R., & Chemashkin, A. V. (2016). Development of feedstock of tungsten-nickel-iron- polyformaldehyde for MIM technology. *IOP Conference Series: Materials Science and Engineering*, 156(1), 12033. doi:10.1088/1757-899X/156/1/012033.
- [11] Myachin, Y. V., Darenskaya, E. A., Vaulina, O. Y., Buyakova, S. P., Turuntaev, I. V., & Kulkov, S. N. (2017). Structure and properties of steel produced by metal injection molding. *Inorganic Materials: Applied Research*, 8(2), 331–334. doi:10.1134/S2075113317020162.
- [12] Vaulina, O. Y., Darenskaia, E. A., Myachin, Y. V., Vasilyeva, I. E., & Kulkov, S. N. (2017). Influence of mechanical activation of steel powder on its properties. *IOP Conference Series: Materials Science and Engineering*, 175(1), 12038. doi:10.1088/1757-899X/175/1/012038.
- [13] Darenskaia, E. A., Vaulina, O. Y., Myachin, Y. V., & Kulkov, S. N. (2017). Influence of binding composition on the structure and properties of steel work-pieces obtained by injection moulding. *IOP Conference Series: Materials Science and Engineering*, 175(1), 12035. doi:10.1088/1757-899X/175/1/012035.
- [14] Parkhomenko, A. V., Amosov, A. P., Samboruk, A. R., Ignatov, S. V., Kostin, D. V., & Shul'timova, A. S. (2015). Development of domestic powder granulate with a polyformaldehyde-based binder for MIM technology. *Russian Journal of Non-Ferrous Metals*, 56(1), 68–72. doi:10.3103/S1067821215010149.
- [15] Momeni, V., Hufnagl, M., Shahroodi, Z., Gonzalez-Gutierrez, J., Schuschnigg, S., Kukla, C., & Holzer, C. (2023). Research Progress on Low-Pressure Powder Injection Molding. *Materials*, 16(1), 379. doi:10.3390/ma16010379.
- [16] Wang, J. (Ed.). (2012). *Some Critical Issues for Injection Molding*. IntechOpen, London, United Kingdom. doi:10.5772/2294.
- [17] Kate, K. H., Onbattavelli, V. P., Enneti, R. K., Lee, S. W., Park, S. J., & Atre, S. V. (2012). Measurements of powder-polymer mixture properties and their use in powder injection molding simulations for aluminum nitride. *JOM*, 64(9), 1048–1058. doi:10.1007/s11837-012-0404-3.
- [18] Kate, K. H., Enneti, R. K., Onbattavelli, V. P., & Atre, S. V. (2013). Feedstock properties and injection molding simulations of bimodal mixtures of nanoscale and microscale aluminum nitride. *Ceramics International*, 39(6), 6887–6897. doi:10.1016/j.ceramint.2013.02.023.

- [19] Kate, K. H., Enneti, R. K., Park, S. J., German, R. M., & Atre, S. V. (2014). Predicting powder-polymer mixture properties for PIM design. *Critical Reviews in Solid State and Materials Sciences*, 39(3), 197–214. doi:10.1080/10408436.2013.808986.
- [20] Archodoulaki, V., & Lüftl, S. (2014). Thermal Properties and Flammability of Polyoxymethylene. *Polyoxymethylene Handbook*, 257–275, John Wiley & Sons, Hoboken, United States. doi:10.1002/9781118914458.ch10.
- [21] Lebedev, S. M., Gefle, O. S., Amitov, E. T., Zhuravlev, D. V., & Berchuk, D. Y. (2018). Thermophysical, Rheological and Morphological Properties of Polyoxymethylene Polymer Composite for Additive Technologies. *Russian Physics Journal*, 61(6), 1029–1033. doi:10.1007/s11182-018-1492-5.
- [22] Durmagambetov, A. (2010). Application of analytic functions to the global solvability of the Cauchy problem for equations of Navier-Stokes. *Natural Science*, 2(4), 338–356. doi:10.4236/ns.2010.24042.
- [23] Weidenfeller, B., Höfer, M., & Schilling, F. R. (2004). Thermal conductivity, thermal diffusivity, and specific heat capacity of particle filled polypropylene. *Composites Part A: Applied Science and Manufacturing*, 35(4), 423–429. doi:10.1016/j.compositesa.2003.11.005.
- [24] Progelhof, R. C., Throne, J. L., & Ruetsch, R. R. (1976). Methods for predicting the thermal conductivity of composite systems: A review. *Polymer Engineering & Science*, 16(9), 615–625. doi:10.1002/pen.760160905.
- [25] Zhu, S., Wu, S., Fu, Y., & Guo, S. (2024). Prediction of particle-reinforced composite material properties based on an improved Halpin-Tsai model. *AIP Advances*, 14(4). doi:10.1063/5.0206774.
- [26] Muranov, A. N., Semenov, A. B., Marakhovskii, P. S., Chutskova, E. Y., & Semenov, B. I. (2019). Thermophysical Properties of Powder-Polymer Mixture for Fabrication of Parts of 42CrMo4 Steel by the MIM Method. *Inorganic Materials: Applied Research*, 10(2), 285–290. doi:10.1134/S207511331902028X.
- [27] Xu, J. Z., Gao, B. Z., & Kang, F. Y. (2016). A reconstruction of Maxwell model for effective thermal conductivity of composite materials. *Applied Thermal Engineering*, 102, 972–979. doi:10.1016/j.applthermaleng.2016.03.155.
- [28] Mamunya, Y. P., Davydenko, V. V., Pissis, P., & Lebedev, E. V. (2002). Electrical and thermal conductivity of polymers filled with metal powders. *European Polymer Journal*, 38(9), 1887–1897. doi:10.1016/S0014-3057(02)00064-2.
- [29] Markov, A. V. (2008). Thermal conductivity of polymers filled with dispersed particles: A model. *Polymer Science Series A*, 50(4), 471–479. doi:10.1134/s0965545x08040160.
- [30] Kowalski, L., Duszczyc, J., & Katgerman, L. (1999). Thermal conductivity of metal powder-polymer feedstock for powder injection moulding. *Journal of Materials Science*, 34(1), 1–5. doi:10.1023/A:1004424401427.
- [31] Wada, Y., Nagasaka, Y., & Nagashima, A. (1985). Measurements and correlation of the thermal conductivity of liquid n-paraffin hydrocarbons and their binary and ternary mixtures. *International Journal of Thermophysics*, 6(3), 251–265. doi:10.1007/BF00522147.
- [32] Wang, J., Xie, H., Guo, Z., Guan, L., & Li, Y. (2014). Improved thermal properties of paraffin wax by the addition of TiO₂ nanoparticles. *Applied Thermal Engineering*, 73(2), 1541–1547. doi:10.1016/j.applthermaleng.2014.05.078.
- [33] Bharathiraja, R., Ramkumar, T., Selvakumar, M., & Radhika, N. (2024). Thermal characteristics enhancement of Paraffin Wax Phase Change Material (PCM) for thermal storage applications. *Renewable Energy*, 222, 119986. doi:10.1016/j.renene.2024.119986.
- [34] Sadaf, M., Cano, S., Bragaglia, M., Schuschnigg, S., Kukla, C., Holzer, C., Vály, L., Kitzmantel, M., Nanni, F., & Gonzalez-Gutierrez, J. (2024). Comparative analysis of binder systems in copper feedstocks for metal extrusion additive manufacturing and metal injection moulding. *Journal of Materials Research and Technology*, 29, 4433–4444. doi:10.1016/j.jmrt.2024.02.163.
- [35] Lim, K., Hayat, M. D., Jena, K. D., Zhang, W., Li, L., & Cao, P. (2023). Interactions of polymeric components in a POM-based binder system for titanium metal injection moulding feedstocks. *Powder Metallurgy*, 66(4), 355–364. doi:10.1080/00325899.2023.2194478.
- [36] Arman, S., & Lazoglu, I. (2023). A comprehensive review of injection mold cooling by using conformal cooling channels and thermally enhanced molds. *International Journal of Advanced Manufacturing Technology*, 127(5–6), 2035–2106. doi:10.1007/s00170-023-11593-w.
- [37] Wang, S. W., Zhang, Y. L., Wu, C., Xiao, L., Lin, G. M., Hu, Y. B., Hao, G. Z., Guo, H., Zhang, G. P., & Jiang, W. (2023). Equal-Material Manufacturing of a Thermoplastic Melt-Cast Explosive Using Thermal-Pressure Coupling Solidification Treatment Technology. *ACS Omega*, 8(18), 16251–16262. doi:10.1021/acsomega.3c00709.
- [38] Yu, M., Qi, L., Cheng, L., Min, W., Mei, Z., Gao, R., & Sun, Z. (2023). The Effect of Cooling Rates on Thermal, Crystallization, Mechanical and Barrier Properties of Rotational Molding Polyamide 11 as the Liner Material for High-Capacity High-Pressure Vessels. *Molecules*, 28(6), 2425. doi:10.3390/molecules28062425.

- [39] Lin, Q., Allanic, N., Mousseau, P., Girault, M., & Deterre, R. (2023). Monitoring and viscosity identification via temperature measurement on a polymer injection molding line. *International Journal of Heat and Mass Transfer*, 206, 123954. doi:10.1016/j.ijheatmasstransfer.2023.123954.
- [40] Alexandrov, I., Malysheva, G., & Guzeva, T. (2012). A Qualitative Visual Analysis of the Fractured Surfaces of Epoxy/Carbon Fibre Composite Prepared by the Melt and the Solution Technologies. 2nd International Conference on Advanced Composite Materials and Technologies for Aerospace Applications, 11-13 June, 2012, Wrexham, United Kingdom.
- [41] Krause, B., & Pötschke, P. (2016). Electrical and thermal conductivity of polypropylene filled with combinations of carbon fillers. *AIP Conference Proceedings*. doi:10.1063/1.4965494.